Magnetotail flows can consume as much solar wind energy as a substorm

T. I. Pulkkinen,[1] E. I. Tanskanen,[1] M. Wiltberger,[2] J. A. Slavin,[3] T. Nagai,[4] G. D. Reeves,[5] L. A. Frank,[6] and J. B. Sigwarth[6]

Received 16 October 2001; revised 17 December 2002; accepted 13 May 2003; published 23 August 2003.

[1] We examine an event on 17 December 1997, during which the Wind and ACE spacecraft measured an extended period of southward interplanetary magnetic field. The high values of the epsilon parameter were interpreted as strong energy input into the magnetotail. Despite this energy input, the polar cap potential and area remained constant over a period of several hours, the inner magnetotail was very quiet, and there were no substorm signatures either in the magnetotail or in the ionosphere. Comparison of data and MHD simulation results show that the energy input to the magnetosphere was enhanced and that this event was not a case where the solar wind monitor would have trouble predicting the interplanetary field reaching the Earth orbit. Both Geotail observations in the tail and the MHD simulations show that a substantial amount of energy was being consumed in the tail flow activity during this period. Order of magnitude estimates indicate that the flows indeed were sufficient to consume the incoming energy in a quasi-continuous even if bursty manner. Observations from the IMAGE meridional magnetometer network reveal that the substorm that followed several hours later was relatively small, and its size was proportional to the energy input after the substorm onset, not to the total energy input since the southward turning of the interplanetary field. It is argued that the continuous flow activity disturbed the formation of the thin current sheet in the inner magnetotail, which led to the delay in the substorm development. However, the controlling factor which finally led to the global instability remains an open issue. *INDEX TERMS:* 2740 Magnetospheric Physics: Magnetospheric configuration and dynamics; 2744 Magnetospheric Physics: Magnetotail; 2753 Magnetospheric Physics: Numerical modeling; 2764 Magnetospheric Physics: Plasma sheet; *KEYWORDS:* magnetotail, substorm, MHD-simulation, flow bursts

Citation: Pulkkinen, T. I., E. I. Tanskanen, M. Wiltberger, J. A. Slavin, T. Nagai, G. D. Reeves, L. A. Frank, and J. B. Sigwarth, Magnetotail flows can consume as much solar wind energy as a substorm, *J. Geophys. Res.*, *108*(A8), 1326, doi:10.1029/2001JA009132, 2003.

1. Introduction

[2] The flow of energy from the solar wind through the magnetosphere-ionosphere system is a key issue in space physics and as such was selected as the main goal of the International Solar-Terrestrial Physics (ISTP) program. However, because of the problems in defining the system by only a few point measurements, and because of the large event-to-event variability of the system, we still lack detailed understanding of the processes related to the energy input-output cycle.

[3] The rate of energy input from the solar wind into the magnetosphere is controlled by the dayside reconnection rate, which is a function of the interplanetary magnetic field (IMF) direction [*Dungey*, 1961; *Fairfield and Cahill*, 1966]. This energy input has been empirically parameterized in terms of the $\epsilon = (4\pi/\mu_0)\, V B^2 l_0^2 \sin^4(\theta/2)$ parameter, which is a function of the solar wind velocity V and the IMF intensity B and direction ($\tan\theta = B_Y/B_Z$) [*Perreault and Akasofu*, 1978; *Akasofu*, 1981]. The energy is consumed in the ionosphere (Joule heating and auroral precipitation) and in the magnetosphere (ring current enhancement, plasma sheet heating), the remaining energy is lost from the magnetotail back to the solar wind (plasmoids) [*Ieda et al.*, 1998; *Kallio et al.*, 2000]. Recent studies have shown that the ionosphere receives the major part of the energy, dissipating at least 50% of the total energy during storms and even more during isolated substorms [*Lu et al.*, 1998; *Tanskanen et al.*, 2002; *Turner et al.*, 2001]. One of the key open issues is whether the relative importance of the various energy channels is constant during different events, or whether the magnetosphere-ionosphere system has many different ways to maintain the energy input-output balance.

[1]Finnish Meteorological Institute, Helsinki, Finland.
[2]Department of Physics and Astronomy, Dartmouth College, Hanover, New Hampshire, USA.
[3]NASA Goddard Space Flight Center, Greenbelt, Maryland, USA.
[4]Department of Earth and Planetary Sciences, Tokyo Institute of Technology, Tokyo, Japan.
[5]Los Alamos National Laboratory, Los Alamos, New Mexico, USA.
[6]Department of Physics and Astronomy, The University of Iowa, Iowa City, Iowa, USA.

0148-0227/03/2001JA009132$09.00

[4] The basic energy loading-release cycle in the magnetosphere is the magnetospheric substorm [e.g., *Baker et al.*, 1996]. In this cycle, energy is first stored in the form of magnetic energy in the tail lobes and later released in an explosive manner when reconnection in the nightside tail leads to large-scale reconfiguration of the magnetospheric fields and plasmas. Several studies have addressed the conditions required for substorm onset to occur; one of the key elements is the formation of a thin and intense current sheet in the magnetotail [e.g., *Pulkkinen et al.*, 1992, *Schindler and Birn*, 1993]. If the driving is very strong, a geomagnetic storm develops [*Burton et al.*, 1975]. The basic distinction between storms and substorms is that storms are associated with a significant intensification of the ring current encircling the Earth mostly inside geostationary orbit [*Dessler and Parker*, 1959; *Sckopke*, 1966]. On the other hand, if the driving is strong and very steady, the magnetosphere can enter into a steady convection configuration [*Sergeev et al.*, 1996], during which there is strong energy dissipation in the ionosphere and flow activity in the tail but no substorms or rapid ring current enhancement. During steady convection periods the large-scale tail field configuration remains stable over a period of several hours, which otherwise is not typical for periods of strong energy input.

[5] The Earthward magnetic flux and plasma transport occur as bursts of localized, high-speed plasma flow. These bursty bulk flows typically have speeds of several hundred km/s, scale sizes of a few R_E, and time scales of about 10 min [*Angelopoulos et al.*, 1992]. Flow bursts are observed during all geomagnetic conditions ranging from quiet to storm time, but their occurrence frequency increases substantially during active times. These bursts can account for a major portion of the Earthward plasma, energy, and flux transport in the magnetotail [*Angelopoulos et al.*, 1994].

[6] The flow bursts in the magnetotail are well correlated with auroral activations in the nightside ionosphere near the satellite footpoint. The flow bursts can correspond to a variety of auroral types such as poleward expansions, pseudobreakups, auroral streamers, or high-latitude activations. If the spacecraft observing a flow burst has its ionospheric footpoint close to the auroral activation, the onset of the flow burst is near-simultaneous with the auroral onset (±1 min, [*Nakamura et al.*, 2000]). In the magnetic data these flow bursts are seen as vortical structures in the ionospheric convection pattern [*Kauristie et al.*, 2000].

[7] The state of the ionosphere can also affect the magnetospheric dynamics. The large Alfvén speed in the ionosphere makes a path via the ionosphere a rapid way to communicate between distant regions of the magnetosphere. The ionospheric drag is a passive resistance on the magnetospheric flows, and the formation of field-aligned current channels requires that the ionospheric electric field and conductivity patterns are consistent with the closure of these currents in the ionosphere. Furthermore, neutral winds can drive field-aligned currents independent of the magnetospheric processes.

[8] As discussed above, the traditional view is that the energy stored in the form of magnetic energy is released by some process (e.g., reconnection) and consumed by Joule heating in the ionosphere, by particle precipitation into the ionosphere, by heating of the plasma sheet, by enhancement of the ring current, or by transporting it back to the solar wind in association with plasmoids. Heating in the collisionless plasma is assumed to occur due to anomalous dissipation caused by wave activity within the plasma sheet. However, two recent studies complement this view by including waves as means of energy transport and dissipation in the magnetosphere-ionosphere system. *Wygant et al.* [2000] showed that the Poynting flux above the auroral acceleration region is much higher than that measured below the acceleration region. They argue that the Poynting flux associated with large-amplitude Alfvén waves is the dominant mechanism for energy transfer from the magnetosphere to the ionosphere and that the energy carried by the Poynting flux is sufficient to power the auroral acceleration related to active auroras. Furthermore, by studying events during weak auroral activity, they also suggest that such intense Alfvén waves are a necessary condition for intense auroras to occur. *Angelopoulos et al.* [2002] examined a flow burst in the magnetotail, the associated wave activity above the acceleration region, and the ionospheric signatures of the flow burst. They conclude that the Poynting flux near the flow burst is much larger than that above the auroral acceleration region but that the energy is still sufficient to power the observed ionospheric activity. These studies would suggest that the Poynging flux is a major means of transporting energy from the magnetosphere to the ionosphere, more important than the field-aligned currents or auroral precipitation.

[9] On the other hand, the *Angelopoulos et al.* [2002] study shows that a substantial amount of the energy is lost between the flow burst and above the auroral acceleration region, i.e., within the plasma sheet. They argue that this energy is dissipated by kinetic Alfvén waves powered by the bursty bulk flow by coupling through flow shear to dawn-dusk flow components. This energy is either consumed by electron heating or radiated out of the flux tube. Thus the large-amplitude waves also provide a means to consume flow burst energy within the plasma sheet through wave-particle interaction or by radiating it away from the flux tube.

[10] Thus all three plasma systems (solar wind, magnetosphere, ionosphere) in part control the type of activity which forms in the magnetosphere. In this paper we examine a period during which, based on the solar wind and IMF parameters, one would have expected a substorm to occur. Instead, the magnetosphere exhibited relatively strong flow activity, which in the ionosphere was seen as auroral activations and small electrojet enhancements. The event ended with a small substorm about three hours later. We examine the driver properties in the solar wind using two spacecraft. We study the magnetotail properties using both magnetotail and geostationary orbit measurements as well as global MHD simulation results. Finally, we discuss the ionospheric properties based on ground-based auroral and magnetic observations.

2. Observations

[11] The event under study occurred on 17 December 1997, 1800–2400 UT. During that time the Wind and ACE spacecraft were both in the upstream solar wind, near the first Lagrangian point L1. More precisely, Wind was at

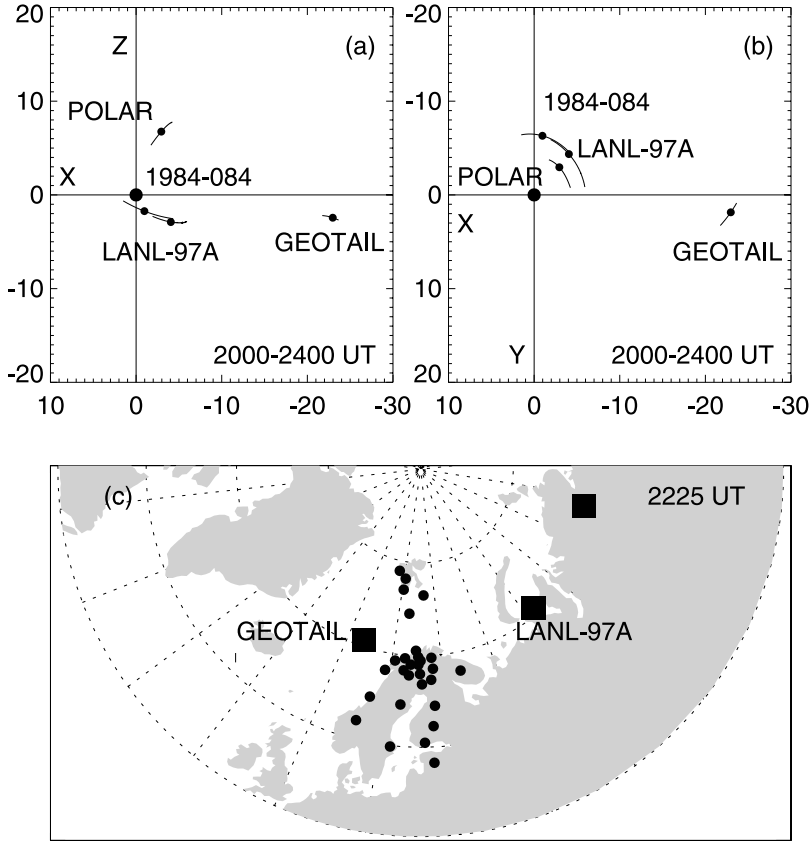

Figure 1. Spacecraft orbits from 2000 UT to 2400 UT (a) in the noon-midnight meridian plane and (b) in the equatorial plane. (c) Ionospheric mapping of the spacecraft positions at 2225 UT (squares) and ground magnetometer network (filled circles).

(214.1, 12.8, 18.3)R_E in geocentric solar-magnetospheric (GSM) coordinates, while ACE was at (210.8, 9.6, −13.8)R_E in GSM coordinates. In the magnetosphere the magnetotail plasma sheet was probed by the Geotail spacecraft, Polar was above the Northern Hemisphere in the high-altitude polar cap, and two geosynchronous spacecraft monitored the energetic particle environment in the early morning sector. Figure 1 shows the satellite locations from 2000 UT to 2300 UT and their ionospheric mappings at 2225 UT. These mappings were made using the *Tsyganenko* [1989] magnetic field model with $Kp = 3$.

[12] Figure 2 shows the solar wind and interplanetary magnetic field parameters as measured by the Wind and ACE spacecraft [*Lepping et al.*, 1995; *Ogilvie et al.*, 1995; *Smith et al.*, 1998]. Figures 2a–2c show the magnetic field components. The B_X and B_Y components are basically similar at both spacecraft, but B_Z exhibits some variability between the two spacecraft. Early in the period, from 1600 UT until 2000 UT, ACE measured slightly more negative B_Z than Wind, whereas between 2000 UT and 2120 UT the opposite was true. Density and velocity measurements were only available from the Wind spacecraft, the density was quite constant around 15 cm^{-3}, and velocity was very steady at slightly below 300 km/s. Figure 2f shows the ϵ parameter computed for the magnetic field measurements at the two spacecraft (Wind plasma measurements were used for ϵ computation for both sets of magnetic field measurements): The results are roughly consistent until about 2140 UT, after which ACE measurements give slightly smaller ϵ values (note that the scale is linear). Owing to the steady solar wind speed, the time delay between the upstream monitors and the Earth can be computed for the entire period of time. Assuming magnetopause location at 10 R_E and a delay time $\Delta X/V$, we obtain 76.8 min for Wind and 75.7 min for ACE.

[13] Figure 3a shows the solar wind energy input as measured by the ϵ parameter delayed to the magnetopause as described above. Figure 3b shows the polar cap index from Thule, and Figures 3c and 3d show the global AU/AL indices and the local night sector IU/IL electrojet indices created from the IMAGE magnetometer network data [*Syrjäsuo et al.*, 1998; *Kallio et al.*, 2000]. Figure 3e shows the polar cap magnetic flux as computed from global auroral images taken by the Polar/VIS Earth camera [*Frank et al.*, 1995], and Figure 3f shows the polar cap magnetic flux as computed from IMP-8 magnetic field measurements assuming a constant 25-R_E radius of the tail. IMP-8 was in the plasma sheet from about 1800 to 2055 UT and in the north lobe the rest of the day. There was a data gap during 2150–2240 UT.

[14] The ϵ parameter data suggest that after 1800 UT the energy input to the magnetosphere was consistently above the substorm limit of 10^{11} W [*Akasofu*, 1981], except for short excursions in the Wind data and one longer excursion in the ACE data. However, the polar cap index [*Troshichev et al.*, 1988; *Vennerstroem et al.*, 1991], started to increase

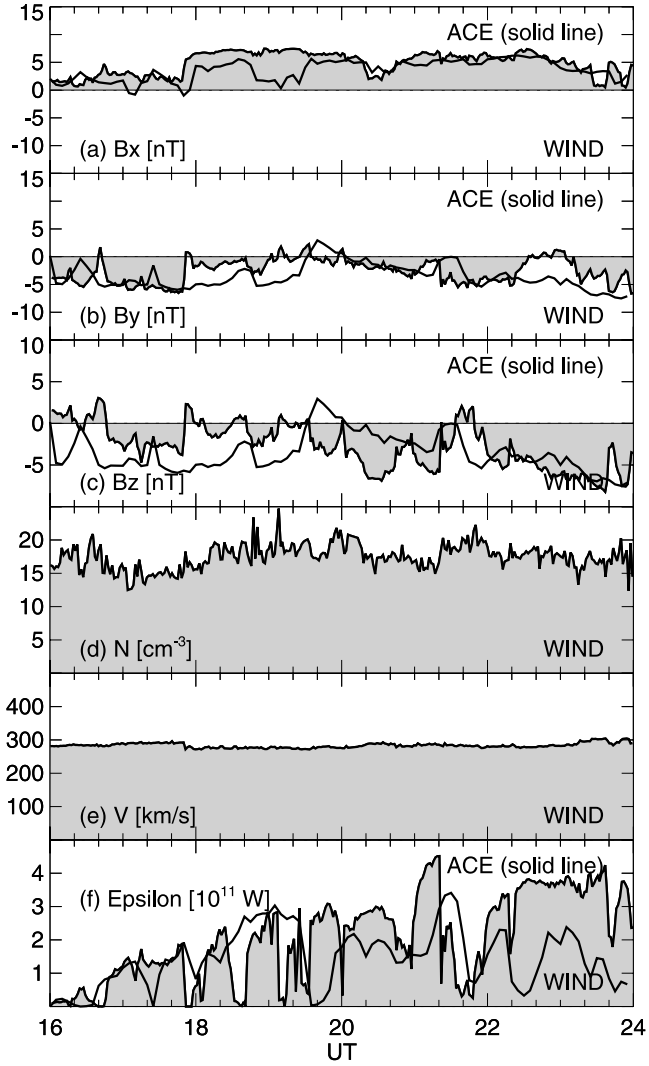

Figure 2. Solar wind and interplanetary magnetic field measurements from Wind and ACE spacecraft. (a) B_X, (b) B_Y, and (c) B_Z from Wind (shaded) and ACE (solid line); solar wind (d) density and (e) velocity from Wind; (f) epsilon-parameter from WIND (shaded) and ACE (solid line).

only after 2030 UT. The polar cap index is composed of near-pole magnetometer data (Thule in the Northern Hemisphere) and gives a measure of the energy input into the magnetosphere if the recording station is in the dayside. However, if the recording station is in the nightside, as was the case for this event, the index increases only when nightside convection has been enhanced [*Cowley and Lockwood*, 1992]. Both the global and night sector electrojet indices suggest that the electrojet enhancement initiated at around 2100 UT and that the following substorm occurred slightly before 2230 UT and had a minimum of only −350 nT in AL. The timing is consistent with the polar cap area (or magnetic flux) behavior, which shows an increase after 2100 UT and a decrease after 2230 UT.

[15] Geotail in the nightside magnetotail observed transient flow activity from about 1800 UT (Figure 4); unfortunately, no magnetic field data were available during this event. The flow direction changed from Earthward to tailward, and the flow velocities were mainly below about 200 km/s. The V_Y component was mainly positive, indicating dawn-to-dusk directed flow component. On the other hand, after 2000 UT there were several distinct bursts of fast flow at 2017–2032, 2047–2110, 2130–2142, and 2220–2245 UT (shown with grey shading in Figure 4). The first flow burst was tailward, the second had both tailward and Earthward components, and the two last ones were earthward directed. The last flow burst followed the substorm onset as seen on the ground. The large dropout in plasma density shows that Geotail went into the tail lobe for a short while. As Geotail reentered the plasma sheet, the Earthward flow velocity recovered simultaneously. This is a classical signature of a plasmoid passing the spacecraft [*Hones et al.*, 1986].

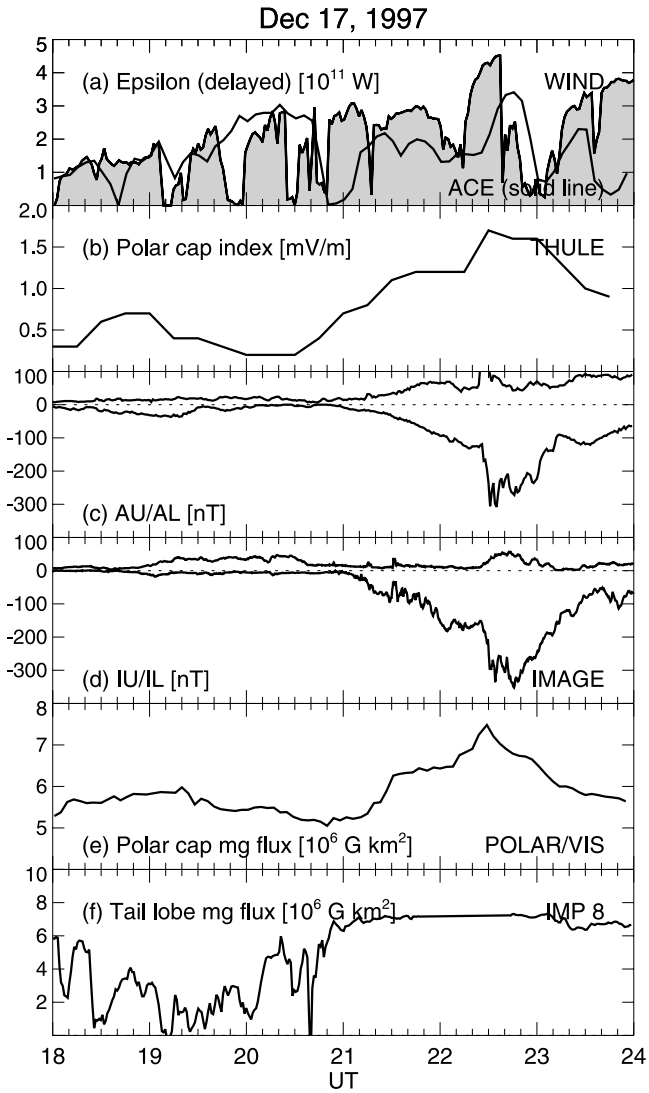

Figure 3. (a) ϵ parameter delayed to the magnetopause from Wind (shaded) and ACE (solid line); (b) Polar cap index from Thule; (c) AU/AL indices; (d) local night sector IU/IL electrojet indices created from the IMAGE magnetometer network data; (e) polar cap magnetic flux derived from Polar/VIS Earth camera images; (f) tail lobe magnetic flux from IMP8.

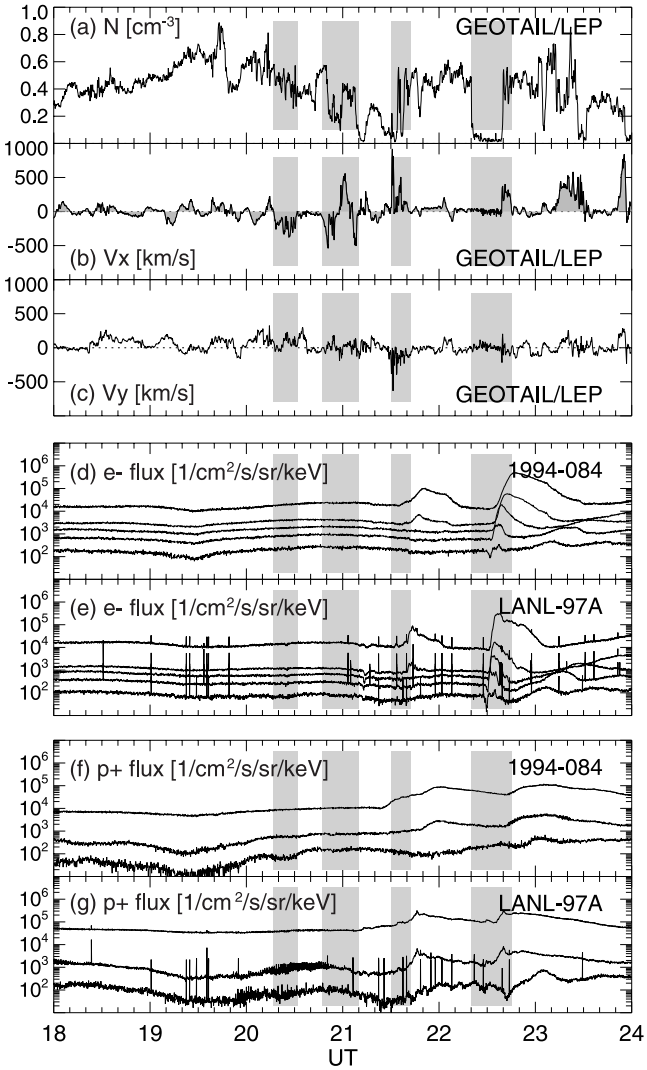

Figure 4. Plasma (a) density and (b)–(c) velocity components from Geotail; differential electron fluxes from (d) s/c 1994-084 and (e) LANL-97A for energy channels 50–75, 75–105, 105–150, 150–225, and 225–315 keV; differential ion fluxes from (f) s/c 1994-084 and (g) LANL-97A for energy channels 50–75, 75–113, and 113–170 keV.

[16] In the geosynchronous magnetotail the period after 1800 UT was very quiet both in terms of electron and proton fluxes (Figure 4). There was a small enhancement in both electrons and protons at about 2130 UT, and a larger (but still moderate) injection at about 2230 UT concurrent with the plasma sheet dropout-Earthward flow event at Geotail. Thus these data suggest that there was a minor activation at 2130 UT and a small substorm at 2230 UT.

[17] Figure 5 shows selected images from Polar/VIS imager during that period. The images were selected to show maximal auroral activity during four brightenings of the oval, each associated with one of the flow bursts. Only the last one was associated with substantial poleward motion of the auroras and hence substorm evolution. In between these brightenings the oval was quiet and no distinct activations were seen.

3. Global MHD Simulation Results

[18] The Lyon-Fedder-Mobarry (LFM) code consists of two interlinked simulations for modeling the solar wind-magnetosphere-ionosphere interaction [*Fedder et al.*, 1995; *Fedder and Lyon*, 1995; *Mobarry et al.*, 1996]. The ideal MHD equations are used to model solar wind and magnetospheric plasmas. The ionosphere is simulated by solving the height-integrated (two-dimensional) electrostatic potential equation that is coupled via field-aligned currents to the magnetospheric simulation.

[19] The MHD equations are solved in a region containing the solar wind and the magnetosphere, in this case a large cylinder 100 R_E in radius and 380 R_E long. Although the ideal MHD equations are nondissipative, the effects of

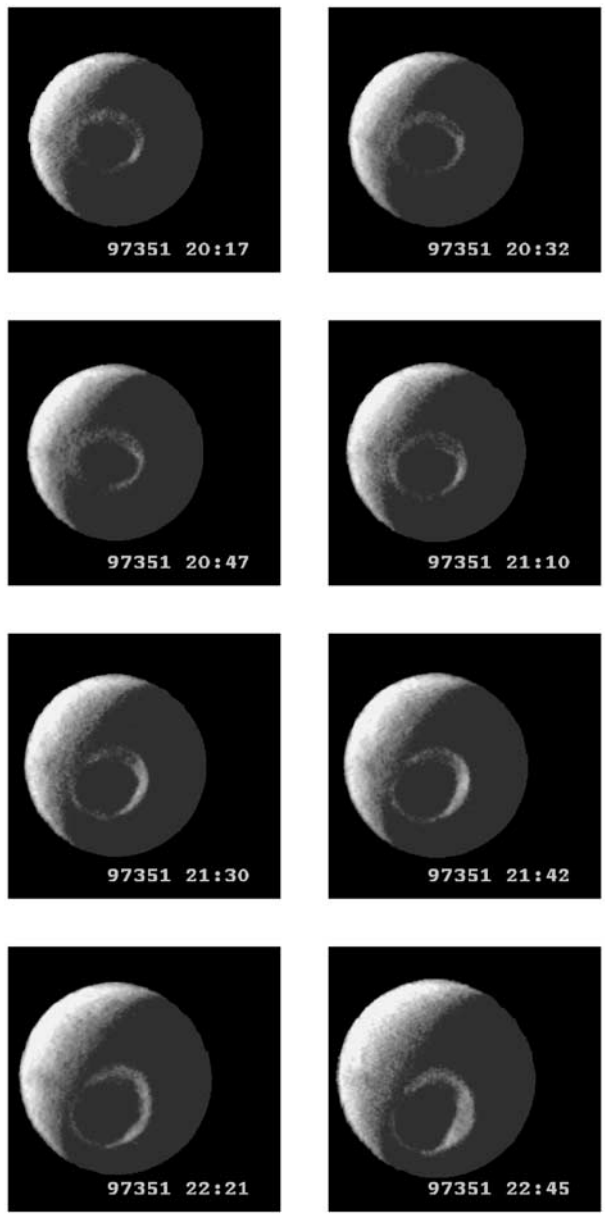

Figure 5. Polar/VIS images of the auroral oval during 17 December 1997. See color version of this figure at back of this issue.

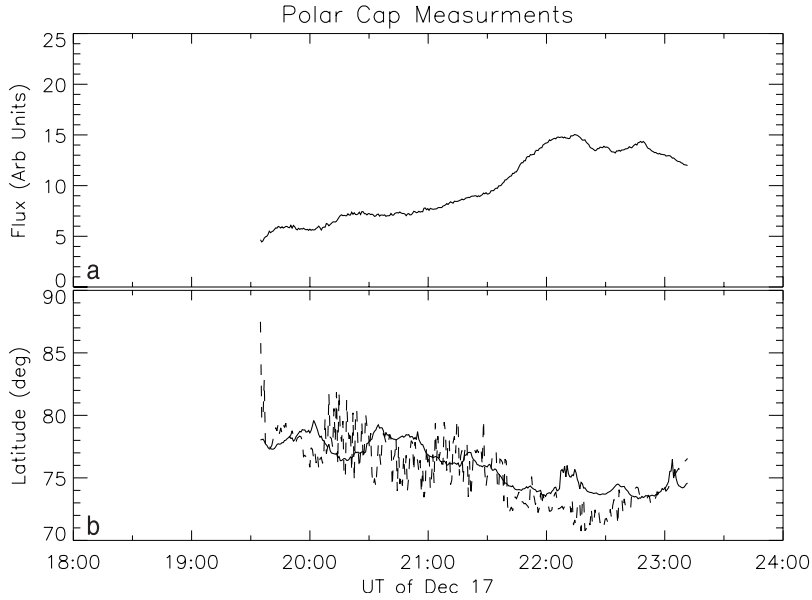

Figure 6. (a) Polar cap magnetic flux in arbitrary units and (b) the poleward boundary of the auroral oval from the global magnetohydrodynamic (MHD) simulation at noon (solid line) and at midnight (dashed line).

finite discretization allow for occurrence of magnetic reconnection. The merging of magnetic fields occurs when oppositely directed magnetic fields convect into a single computational cell and the numerical averaging within the cell results in annihilation of the magnetic flux. The resulting numerical resistivity is important only in regions where this forced reconnection occurs, and the reconnection rate is largely controlled by the external boundary conditions [*Fedder et al.*, 1995]. Furthermore, grid resolution is not controlling the reconnection rate [*Wiltberger et al.*, 2000].

[20] The simulation code was run for the 17 December 1997 event during 1800–2400 UT, using the Wind measurements as boundary conditions to the simulation. In order to keep the magnetic field divergenceless, the B_X component is given as a liner combination of the other two components, $B_X(t) = a + bB_Y(t) + cB_Z(t)$, which results in a good fit with the actually measured B_X component using the constants $a = 6.18878$, $b = 0.9873$, and $c = 0.03252$.

[21] Figure 6 shows the polar cap magnetic flux and the poleward boundary of the auroral oval from the simulation over the period of interest, from 1930 until 2315 UT. The polar cap magnetic flux increased slowly between 1930 and 2130 UT, after which a more distinct increase followed. The polar cap flux varied around a constant level, and started to decrease after 2300 UT. The poleward boundary of the auroral oval (bottom panel) was variable but approximately constant during 1930–2130 UT, after which it decreased until after the substorm expansion phase it started to increase again. The size of the auroral oval, as depicted here in the form of the latitude of the poleward boundary at noon and midnight, is a good indicator of the amount of energy storage in the tail lobe magnetic energy. The relatively constant locations of the boundary until about 2130 UT indicates that most of the energy that entered the magnetosphere was being continuously consumed by the system.

[22] In the magnetotail the period from 1930 to 2115 UT was characterized by gradual compression of the plasma sheet, distinct lobes void of plasma, and Earthward plasma flow throughout the inner and middle magnetotail out to 50 R_E. At 2245 UT there was a large-scale reconnection event and a plasmoid release with a near-Earth neutral line at about 25 R_E.

[23] In the current sheet plane, more and much smaller-scale activity was recorded. Figure 7 shows the approximate current sheet plane with electric field intensity color coded and flow velocity vectors overlaid. During 1930–2025 UT the cross-tail current enhanced slowly, but the large-scale electric field was small. The first flow channel formed around 2025–2036 UT in the evening sector. Tracing back in the simulation, the first signatures of a very weak electric field enhancement were observed at 2009 UT, but it was not until 2025 UT that the flow velocities increased substantially. This burst did not reach the inner magnetosphere and did not disturb the current sheet that had formed near the inner edge of the plasma sheet (from inside 10 R_E to about 20 R_E).

[24] A second flow burst was seen in the simulation only about 10 min later at 2040–2050 UT. This burst occurred near the tail center, but slightly in the premidnight sector. Flows at this time reached inside of 10 R_E, and the inner edge current pattern was disturbed but not completely disrupted.

[25] Following that, there were several activations of a flow channel that formed in the evening sector first at 2105 UT. The bursts occurred at 2105–2120 UT, 2125–2140 UT, and 2150–2200 UT, thus each lasting 10–15 min. Simultaneously, an intense current sheet began to develop at the inner edge of the plasma sheet, and the current sheet remained intense until about 2220 UT, surviving the flow activity until the global-scale activation initiated. After 2220 UT, a large-scale flow pattern formed with Earthward flows inside of 25 R_E and tailward flows tailward of 25 R_E. During the following hour, the inner edge current was disrupted and the inner tail magnetic field was dipolarized,

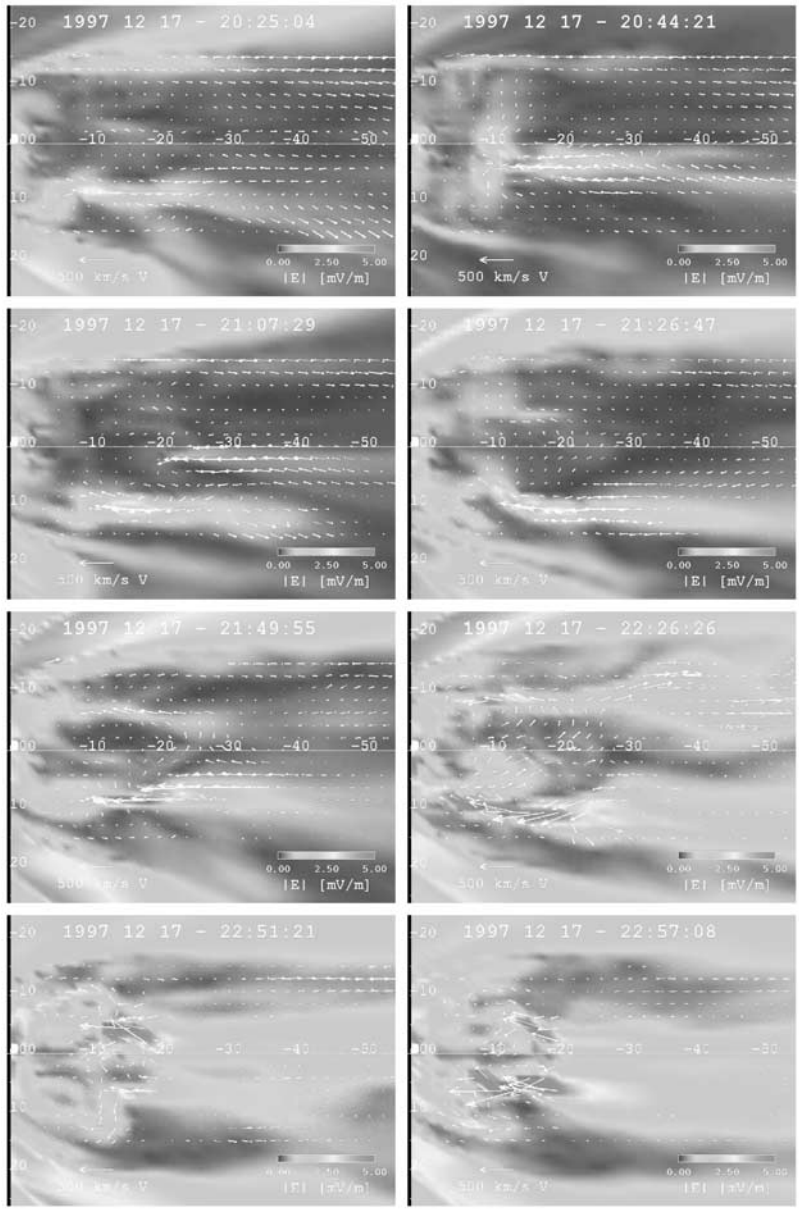

Figure 7. Electric field in the plane $Z = -3.5\ R_E$ from the MHD simulation. The white arrows show the flow velocity projected to the equatorial plane. Time runs from left to right and from top to bottom, the frames are taken at 2025, 2044, 2107, 2126, 2149, 2226, 2251, and 2257 UT. See color version of this figure at back of this issue.

and the entire magnetotail was reconfigured. This occurred coincident with the decrease of the polar cap flux and poleward motion of the auroral oval boundary as shown in Figure 6.

[26] The simulation results are quite consistent with the observations, showing flow activity after the onset of energy input, several flow bursts during 2030–2230 UT, and a global substorm onset after 2230 UT.

4. Energy Dissipation Versus Storage During the Growth Phase

[27] There were no growth phase or expansion phase signatures during 1800–2100 UT. The polar cap area was constant, electrojet indices showed no activity, and the inner magnetosphere showed no injections or other disturbances. This indicates that the energy, if it entered the magnetosphere, was consumed within the plasma sheet and/or high-latitude ionosphere instead of being stored as lobe magnetic energy.

[28] Both Geotail observations (Figure 4) and the MHD simulation results (Figure 7) show that there was substantial flow activity in the magnetotail during the period of energy input. Narrow flow channels were created around or tailward of 50 R_E in the tail, and at times the flows penetrated to the inner magnetosphere disturbing the formation of the thin current sheet in the inner magnetotail. The flow velocities in the flow bursts were quite large, but their cross-tail width remained small. It was not until 2240 UT when a large-scale flow channel and a large-scale neutral

line formed and led to the substorm onset and global reconfiguration of the inner magnetotail.

[29] The frequent occurrence of the magnetotail flows is a clear signature that energy was being deposited into the magnetosphere; typically during quiet times the flow burst occurrence rates are much smaller [*Angelopoulos et al.*, 1994]. Thus it is unlikely that the relatively strongly southward IMF observed by two spacecraft in the interplanetary medium would have missed the magnetosphere. The similarity of the global evolution in the observations and in the simulation results is further evidence for the energy input. The simulation uses the solar wind input throughout the outer boundary in the dayside. Therefore the solar wind that was measured at Wind (and used as simulation input) did encounter the magnetosphere in the MHD simulation. If in reality the IMF at the dayside magnetopause would have been markedly different, this should have led to clearly different temporal evolution of the simulation and observations, which was not the case.

[30] The IMP 8 spacecraft entered the lobe from the plasma sheet around 2055 UT. This is most likely due to the plasma sheet thinning associated with lobe flux loading. The lobe field before 1800 UT (data not shown) was about 16 nT, while at 2130 UT the lobe field was just under 19 nT. Thus the onset of flux loading into the tail after 2100 UT is consistent with the IMP 8 observations.

[31] We are then left to conclude that the energy that was deposited in the magnetotail during 1800–2100 UT was being continuously consumed by plasma sheet processes in the middle magnetotail region between 10 and 50 R_E. The flow channels in the MHD simulation were typically about 5–7 R_E wide (although this value could be overestimated by the relatively poor spatial resolution of the MHD simulation), and their lengths were of the order of 30–40 R_E. Typical electric field values were of the order of 2 mV/m, with higher values in localized maxima and lower values at the trailing edges of the flow channels. Typically, the current densities in the tail in the simulation were about 1 nA/m^2. Assuming such large dimensions ($30 \times 5 \times 2\ R_E{}^3$), and that elecctromagnetic energy was transformed to plasma energy throughout the flow channel by $\mathbf{E} \cdot \mathbf{j}$, the power in each flow channel was roughly $1.5 \cdot 10^{11}$ W, and during a 10-min flow burst about 10^{14} J would have been consumed. These numbers are about 10 times larger than those obtained by *Angelopoulos et al.* [1994], which is a direct consequence of the assumed larger size of the flow channels based on the MHD simulation results. On the other hand, as the energy input rate was of the order of a few times 10^{11} W, the rate of energy dissipation during frequently occurring large-scale flow bursts was quite sufficient to consume a substantial amount of the energy coming into the magnetosphere. Furthermore, if there was substantial wave activity associated with the flow bursts, part of the energy could be consumed by kinetic Alfvén waves [*Angelopoulos et al.*, 2002].

5. Directly Driven Versus Loading-Unloading Processes in the Magnetosphere

[32] It has long been recognized that substorms consist of both a directly driven component and a loading-unloading component [e.g., *Baker et al.*, 1984]. The directly driven process is associated with the enhancement of (ionospheric) convection after the southward turning of the IMF that is observed with a time delay of about 20 min [*Bargatze et al.*, 1985]. On the other hand, the loading-unloading process is related to a reconfiguration process in the magnetotail, where a large amount of energy is explosively released and dissipated in the ionosphere, inner magnetosphere, and magnetotail. This process typically initiates after about 60 min of southward IMF and has been successfully described as a nonlinear system where the energy release occurs after some critical conditions have been reached in the magnetosphere or after some critical amount of energy input [e.g., *Klimas et al.*, 1994]. Nonlinear models utilizing the energy storage and consequent dissipation have reached remarkable prediction capability using past and present solar wind and IMF measurements as input to the nonlinear models [e.g., *Vassiliadis et al.*, 1995].

[33] Based on the results reviewed above, it is often assumed that the energy released during the substorm expansion phase is proportional to the amount of energy stored in the magnetotail during the substorm growth phase. However, a recent study by *Kallio et al.* [2000] indicates that this is not necessarily the case. Statistical examination of the energy input during the substorm growth, expansion, and recovery phases (as evaluated from the time integral of the ϵ parameter) and energy dissipation in the ionospheric Joule heating (as evaluated from the night sector electrojet activity) shows that whereas the energy dissipation in the ionosphere shows no correlation with the energy input during the growth phase, there is a good correlation between the energy dissipation in the ionosphere and the energy input during the substorm expansion and recovery phases. From this study, *Kallio et al.* [2000] concluded that the growth phase energy input is necessary for the reconfiguration of the magnetosphere to a state where a global instability can develop but that it is really the energy input after the substorm onset that determines the "size of the substorm" as measured by electrojet activity in the ionosphere. Thus the role of the growth phase is to reconfigure the magnetotail to a state where a global instability can occur. The size of the substorm (and hence the amount of energy consumed in the ionosphere) is controlled by the energy input after the expansion phase onset.

[34] In addition to Joule heating, the auroral precipitation is a major energy sink during magnetospheric activity. These two are temporally well correlated [*Lu et al.*, 1998], but the latter is usually at least a factor of two smaller. However, during times of only weak auroral precipitation and no major electrojet enhancement, the energy carried by the precipitating particles can become equal to the energy associated with the ionospheric Joule heating. Thus during small events the typical assumption of Joule heating as the dominant energy dissipation mechanism may not hold, but it can be assumed that the energy in the auroral precipitation does not exceed the Joule heating by large amounts. This is equivalent to assuming that intense auroral precipitation is always accompanied by significant ionospheric electrojet activity.

[35] With the above aspects in mind, we compare four substorms with the event described in this paper. Figure 8 shows the energy input (as evaluated from the time integral of the ϵ parameter) and the energy output by dissipation

through ionospheric Joule heating (as evaluated from the time integral of the local *I L* index, see *Kallio et al.* [2000]) for substorm events on 12 January 1997 (AL_{MAX} = 1250 nT), 10 December 1996 (AL_{MAX} = 900 nT), 16 December 1996 (AL_{MAX} = 300 nT), 24 January 1997 (AL_{MAX} = 175 nT), and 17 December 1997 (AL_{MAX} = 350 nT) (see *Pulkkinen et al.* [1998] for description of the first four events). Three values of energy input are shown: energy input during the growth phase (Figure 8a, $\int \epsilon dt_{GROWTH}$), energy input during the expansion and recovery phases (Figure 8b, $\int \epsilon dt_{EXP}$), and energy input during the entire substorm (Figure 8c, $\int \epsilon dt_{TOT} = \int \epsilon dt_{GROWTH} + \int \epsilon dt_{EXP}$)). The energy input or the time integral of the epsilon parameter is given in units of 10^{15} J, whereas the energy dissipation or the time integral of the local *I L* index is given in units of 10^6 nTs (which can be scaled to energy units using the scaling factor $3 \cdot 10^8$ J/nT as suggested by *Ahn et al.* [1983]). In Figure 8a, the mean value of four events, excluding the event of 17 December 1997 (circled), is shown by the vertical line. The solid line in Figure 8b shows the least squares fit to all data points; the correlation coefficient is 0.95. Figure 8c shows a similar fit, but now again excluding the (circled) event of 17 December 1997. The horizontal dashed lines highlight the fact that for each event, the vertical axis values are the same in each of the diagrams.

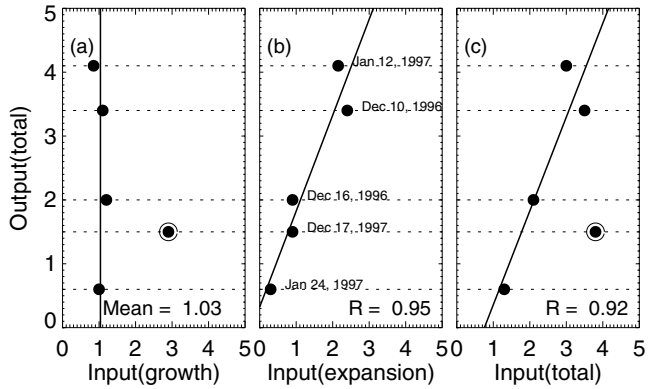

Figure 8. Energy input ($\int \epsilon dt$) versus energy output ($\int ILdt$) for substorm events on 12 January 1997, 10 December 1996, 16 December 1996, 24 January 1997, and 17 December 1997. (a) $\int \epsilon dt_{GROWTH}$ versus $\int ILdt_{TOT}$. Solid line shows the mean value for the four events (excluding the circled one). (b) $\int \epsilon dt_{EXP}$ versus $\int ILdt_{TOT}$. The solid line shows a linear fit to all five data points. (c) $\int \epsilon dt_{TOT} = \int \epsilon dt_{GROWTH} + \int \epsilon dt_{EXP}$ versus $\int ILdt_{TOT}$. The solid line shows a linear fit to the four data points excluding the circled one.

[36] Except for the event on 17 December 1997 (shown circled), the energy input during the growth phase is approximately constant, and around the level of 10^{15} J. During the 17 December 1997 event the energy input during the growth phase was almost three times larger before the substorm onset occurred. Comparison of the energy input and dissipation during the substorm expansion and recovery phases (Figure 8b) shows a good correlation with a correlation coefficient of 0.95 for all events, including the 17 December 1997 event. When the total energy input and dissipation are compared, the 17 December 1997 event is again outside the linear trend. Considering only the four events (excluding 17 December 1997) for the fit, the correlation coefficient is slightly lower, 0.92.

[37] It can be concluded that the expansion and recovery phases of the substorm on 17 December 1997 were typical and had a size that was determined by the amount of energy input after the substorm onset. The good correlation of the substorm size and expansion and recovery phase energy input shows that the energy stored during the growth phase indeed went to the tail reconfiguration, and played little role in the size of the substorm that followed.

[38] It is also clear that the energy input during the growth phase of the 17 December 1997 event is large as compared to the other events. Such events are not exceptional but not very common either. The statistical study by *Kallio et al.* [2000] demonstrates that the growth phase contribution is approximately constant, but its variability does not affect the size of the substorm that follows.

[39] Energy storage estimates can be made either from local magnetotail lobe magnetic field measurements (Figure 3f) or by global images of the auroral precipitation (Figure 3e). Both methods suffer from uncertainties. The magnetic field measurements are accurate, but one needs an assumption of the tail radius to estimate the total flux. The auroral images give a global representation, but the open-closed fieldline boundary is not necessarily equivalent to the poleward boundary of the auroral precipitation. Especially, it has been shown that the auroral precipitation exhibits stroger variability during substorms than the open-closed boundary as measured by direct ion precipitation measurements [*Kauristie et al.*, 1999].

[40] In this event, generally the flux estimates from both methods agree, but the variability in the tail lobe measurements is much smaller than that recorded by the Polar imager. The Polar measurements suggest an increase from the minimum to maximum of about 50%, while the IMP 8 measurements indicate a rise of only about 20%. Furthermore, the MHD simulations indicate an almost factor of 2 rise in the polar cap flux during the growth phase but shows much weaker decrease after the substorm expansion. There are many possible explanations for the differences between the Polar and IMP 8 measurements: The imager records light emitted by atoms created by collisions with precipitating particles. Both sufficient number of particles and particles of sufficiently large energy are required before auroral light is created in amounts that can be detected by the camera. Thus the instrument may miss a portion of the high-latitude/distant tail plasma sheet and thus overestimate the size of the polar cap. On the other hand, the growth phase can cause changes in the tail flaring angle as well as the tail radius, which both would lead to underestimation of the flux changes made from magnetic field measurements. It is also possible (and likely) that IMP 8 maximum flux was reached during the data gap. The large changes in the MHD simulation polar cap flux are largely caused by the inward motion of the distant neutral line during southward IMF, which is a characteristic of all MHD simulations.

[41] The magnetic field measurements in the tail lobe are also an indication of plasma transport within the plasma sheet: the traveling compression regions (TCRs) are indicative of a plasmoid passing the spacecraft location [*Slavin et al.*, 1993]. It is interesting to note that after the substorm, the Earthward flow burst at 2313–2330 UT is very similar in

onset timing and duration to the flux decrease at IMP 8. This would imply a plasma sheet expansion (not reaching the IMP 8 location), Earthward transport of plasma, and weakening of the substorm-associated current system.

6. Substorms in MHD Simulations

[42] In this section we briefly comment on the global MHD simulation results and compare them with simulations of other substorm events. Especially, we concentrate on the growth phase evolution, on the thin current sheet dynamics, and on the issues related to the temporal and spatial scales of the substorm-associated processes in the magnetotail.

[43] The energy enters the magnetosphere mainly in the form of Poynting flux if there is a component of the magnetic field normal to the magnetopause, i.e., after dayside reconnection has opened the magnetopause [*Papadopoulos et al.*, 1999; *Palmroth et al.*, 2002]. After entering the magnetosphere the Poynting flux is transported toward the plasma sheet, as dictated by the magnetic and electric field geometries. As the Poynting flux depends only on the open magnetopause topology and tail geometry, the behavior during typical substorms [*Papadopoulos et al.*, 1999] and during the event studied in this paper would be quite similar.

[44] In the event studied in this paper the polar cap area and the polar cap magnetic flux increased only slowly for about 2 hours after the southward turning of the interplanetary field and hence after the onset of dayside reconnection. This is clearly different behavior from other studied events: *Lopez et al.* [1999] show the polar cap boundaries for the 9 March 1995 substorm event. In that case the dayside boundary started to move equatorward immediately after the southward turning, and the nightside boundary followed after about 15 min delay. During 45 min the change in the boundary locations for both dayside and nightside was about 10° in latitude. This behavior was coincident with rapid increase of the polar cap magnetic flux [*Lyon et al.*, 1998]. *Pulkkinen and Wiltberger* [1999] show only the polar cap flux, but its increase started within a few minutes after the arrival of the southward IMF at the magnetopause; similar results were obtained by *Raeder et al.* [2001] for a substorm event on 24 November 1996. Thus it seems that the magnetospheric response to the IMF southward turning during the 17 December 1997 event studied here is markedly different from other simulated substorm events. As strong flow bursts were not associated with the growth phases of the other substorm events, we further assert that the flow bursts indeed were the means by which the energy was dissipated as it entered the magnetosphere.

[45] The evolution of the magnetotail current sheet was studied in detail by *Pulkkinen and Wiltberger* [2000] for the substorm event on 10 December 1996. They found that during the growth phase, there was a gradual evolution in the inner magnetotail that led to thinning and intensification of the cross-tail current sheet in the region roughly between 10 and 20 R_E in the tail. The current sheet thickness before the substorm onset was less than 1 R_E (near simulation resolution), and the current density had increased by more than a factor of 5 from the pregrowth phase situation. In the event studied here the current sheet evolution was disturbed by the intruding flow channels, and thus the current sheet remained thicker and the current intensity lower than during the 10 December 1996 substorm event. Figure 9 shows a comparison of the current densities in both noon-midnight and equatorial planes for times near the substorm onset for the 10 December 1996 substorm event and for the 17 December 1997 event. Even by the substorm onset, the current density in the 17 December 1997 event did not reach values that were obtained during the more typical substorm event. Thus we assert that the flow bursts, by disturbing the formation of the thin current sheet in the inner tail, not only provided means for energy dissipation but also provided a mechanism to maintain tail stability during the extended period of southward IMF.

[46] The flow burst sizes described in this paper were quite limited, about $5-7$ R_E in cross-tail dimension, and we suspect that if the simulation resolution was higher, the flow channels could be even narrower. Furthermore, the flow channels formed in all parts of the tail, as well near midnight, as in the dawn and dusk sectors. This is distinctly different from the flows associated with substorm onsets. Both *Raeder et al.* [2001] and *Pulkkinen and Wiltberger* [2000] show that the Earthward flow front was more than 10 R_E wide and centered near midnight. Thus the flow channels that probably were created by bursts of reconnection in the midtail are quite different in character to the flows observed at substorm onset: reconnection associated with the flow formation is further out than during substorms, the flow reversal regions (reconnection sites) are more limited in Y, and the locations in Y are more variable than during the global substorm onsets.

[47] In order to examine the energetics during these two events in more detail, the energy content variations in the magnetotail were examined during the two events. Figure 10 shows the energy contents within a central portion of the tail, ± 5 R_E in both Y and Z directions, centered at $X = Z = 0$, for four distances in the downtail direction: $-5 > X > -15$, $-15 > X > -25$, $-25 > X > -35$, and $-35 > X > -45$ R_E. The thermal, kinetic, and magnetic energy contents were integrated over these volumes, and are depicted in Figure 10 with solid, dashed, and dash-dotted lines, respectively. Figure 10a shows the energy contents for the event discussed in this paper (17 December 1997), and Figure 10b shows the energy contents for the substorm event on 10 December 1996. In order to show the temporal changes for all energies, the averages over the time period have been subtracted from the figures.

[48] For both events, most of the energy content variations are concentrated in the inner parts of the magnetosphere, inside 25 R_E. For the 17 December 1997 case it is evident that the magnetic energy stayed relatively constant until about 2100 UT when the growth phase started and then increased until the global instability onset somewhat after 2200 UT. The kinetic energy shows a decrease after 2100 UT, which probably is due to the fact that the plasma sheet is thinning throughout the growth phase period, becoming very thin after the main onset after 2200 UT. The thermal energy content increased throughout the interval until the main onset when the thermal energy began to decrease.

[49] The substorm event on 10 December 1996 (Figure 10b) showed growth phase-associated increase of the magnetic energy from before 0700 UT until the global reconfiguration after 0800 UT. In this case the kinetic energy remained relatively constant, decreasing only after the

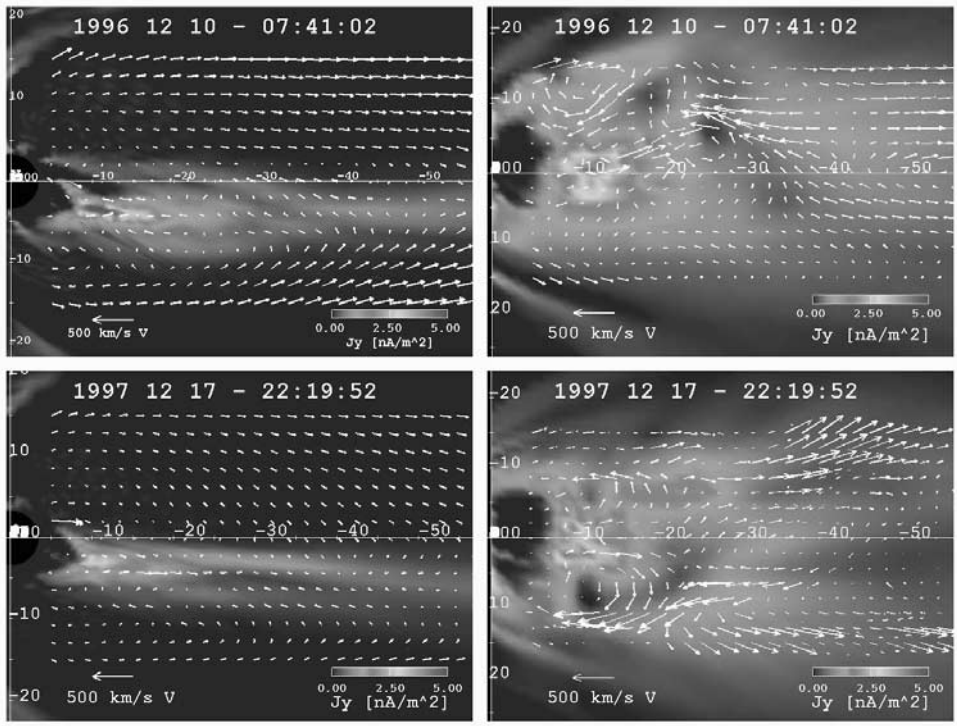

Figure 9. Electric current density in the (left) noon-midnight plane and in the (right) $Z = const$ plane near the plasma sheet center for (top) 10 December 1996 substorm event and (bottom) 17 December 1997 event. See color version of this figure at back of this issue.

global onset after 0800 UT. Again, the thermal energy increased throughout the period of southward IMF, but in this case already the small onset that took place at 0730 UT [see *Pulkkinen and Wiltberger*, 2000] led to reduction of the thermal energy.

[50] Comparison of Figures 10a and 10b leads us to conclude that southward IMF in the simulation leads to increase of the plasma thermal energy if there are no major dissipation events. While during the substorm event on 10 December 1996, the plasma kinetic energy increased slowly throughout the event, during the event on 17 December 1997, the kinetic energy was at a higher level during the period of the flow burst activity and reduced to lower level after the growth phase onset. On the other hand, during the substorm on 10 December 1996, the magnetic energy began to grow soon after the IMF southward turning, while during the 17 December 1997 event the magnetic energy was relatively constant until about 2100 UT, after which the flow energy began to decrease and magnetic energy to increase.

[51] In conclusion, the energetics of the 17 December 1997 event is different from a substorm event: during the period of strong flow activity the southward IMF did not lead to increase of the tail magnetic energy content and the energy was consumed as plasma kinetic energy. However, it is still unclear which process led to the change from the flow activity to the more typical growth phase behavior and magnetic energy storage around 2100 UT.

7. Discussion and Conclusions

[52] In this paper we have examined a period during which energy was deposited into the magnetosphere and quasi-continuously consumed by magnetotail flows. This phase lasted about 3 hours. Following that, a substorm growth phase commenced, and a small substorm took place another 1.5 hour later. Thus the magnetosphere clearly exhibited two different types of behavior: direct energy dissipation by flow activity and energy storage-release during the substorm period.

[53] Accurate evaluation of the energy input from the solar wind to the magnetosphere is problematic, as it is done using point measurements from a spacecraft far away from the magnetopause and well upstream of the bow shock. Magnetic structures in the solar wind have a scale size of several tens of R_E, numbers between 50 and 150 R_E have been suggested [*Crooker et al.*, 1982; *Paularena et al.*, 1998]; this can potentially cause differences especially when the solar wind monitor is far away from the Sun-Earth line. Furthermore, solar wind-foreshock-bow shock interaction can create pressure variations that affect the magnetospheric dynamics in a way not predictable from the upstream monitor [*Fairfield et al.*, 1990]. However, in our event the results are similar (although not equivalent) for two upstream spacecraft, and the ionospheric data also indicates that energy is indeed transferred into the magnetosphere thus supporting our estimates of the energy input.

[54] During periods of steady magnetospheric convection the magnetotail arrives at a quite similar balance than during this event: flow activity in the tail, auroral activity in the ionosphere, and no clear substorm evolution. However, there are also features that distinguish this event from steady convection events. The electrojet activity was extremely weak even though a meridional chain was directly underneath the observed auroral activations. The inner magneto-

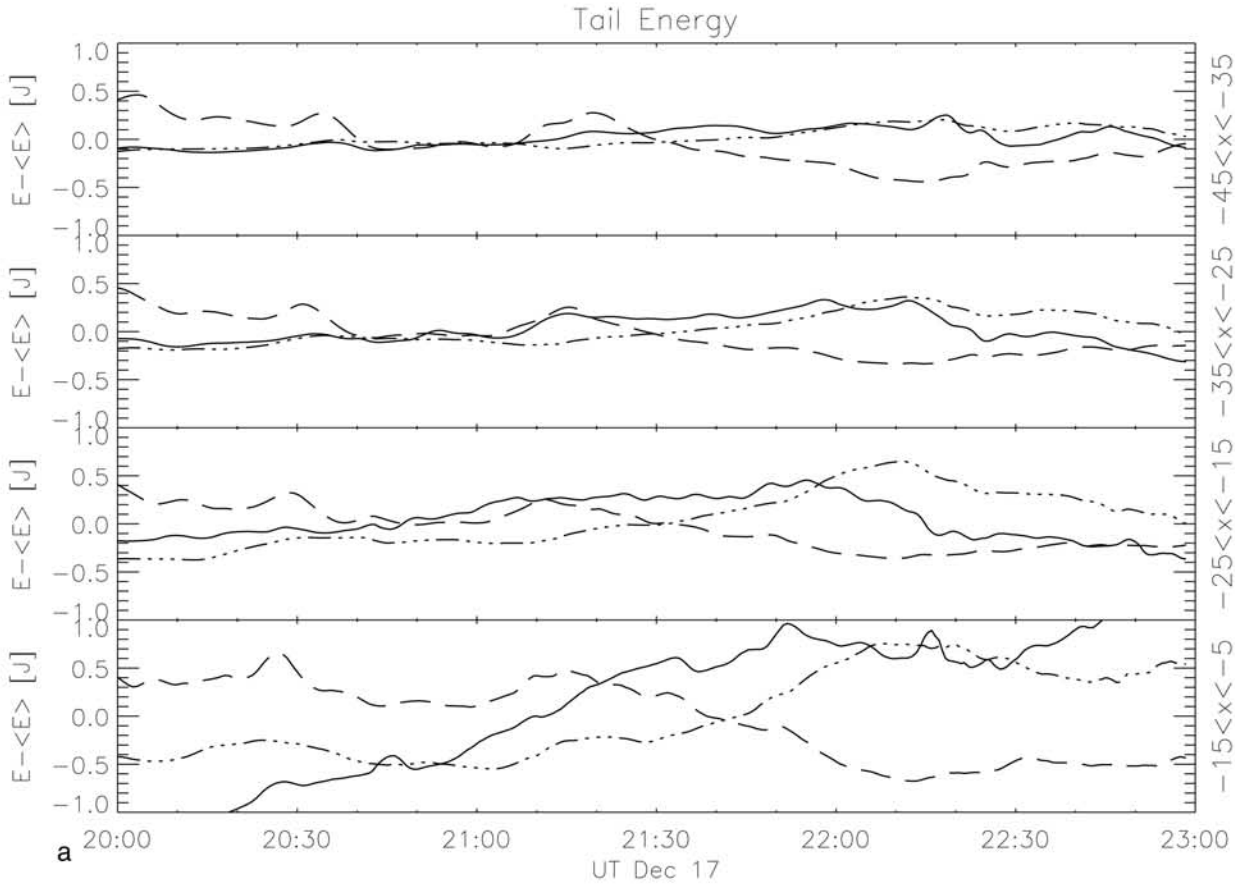
Tail Energy
E−<E> [J]
−45<x<−35
−35<x<−25
−25<x<−15
−15<x<−5
20:00
20:30
21:00
21:30
22:00
22:30
23:00
UT Dec 17
a

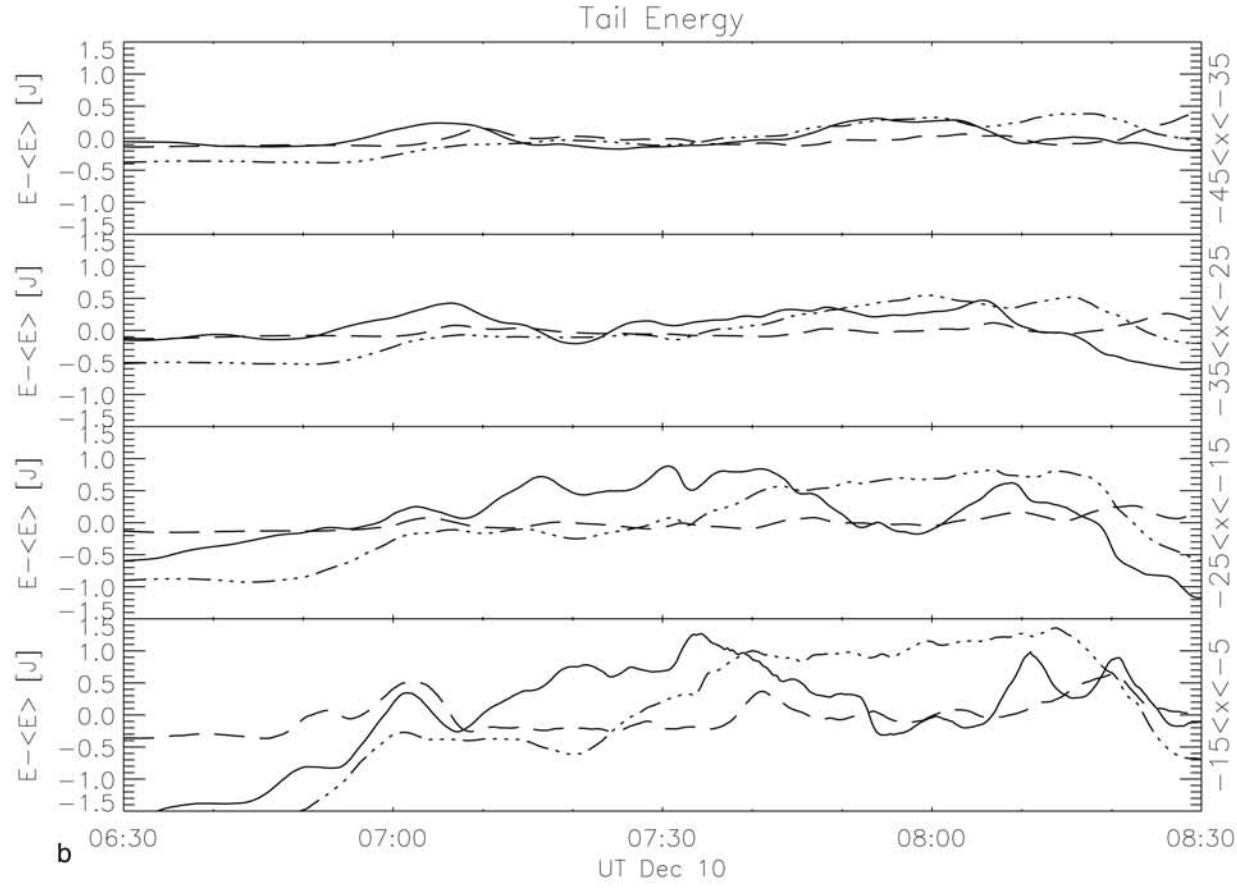
Tail Energy
E−<E> [J]
−45<x<−35
−35<x<−25
−25<x<−15
−15<x<−5
06:30
07:00
07:30
08:00
08:30
UT Dec 10
b

sphere was very quiet and showed no development of a thin current sheet. Lastly, even though the solar wind velocity and density were very steady, the IMF was quite variable, which usually is sufficient to prohibit the formation of steady convection events. Thus it is concluded that this event shared features with but is distinct from steady convection events.

[55] The MHD simulation results clearly show that the thin current sheet development in the inner magnetotail was disturbed by the flow activity. As the flows intruded into the inner magnetosphere, the current sheet was locally disrupted, and a very thin and intense structure typical of the substorm growth phases did not develop. This factor contributed to the delay in the substorm development. On the other hand, the flow channels were strong enough that they could easily consume the energy that was deposited in the magnetosphere by the solar wind-magnetosphere interaction. Thus the substorm growth phase did not develop as the inner tail could not form a thin current sheet and the energy was directly consumed by the flow activity.

[56] The magnetic activity in the ionosphere was at very low level until about 2100 UT. The global AL/AU indices were below 50 nT, and the local magnetometer network showed only very weak electrojet activity before about 2100 UT, after which the westward electrojet started a quasi-continuous increase before the substorm onset at 2230 UT. Both during the quiet period and during the enhancing westward electrojet there were several auroral brightenings that took place overhead the magnetometer chain. These auroral activations (whose maxima are shown in Figure 5) each lasted about 10–15 min but, with the exception of the last event at substorm onset, did not lead to poleward motion of the auroras. It seems that the auroral brightenings were associated with soft precipitation, which did not lead to strong electrojet enhancement in the ionosphere. The flow activity was thus associated with auroral brightenings, which however were not substorm expansions. The weak auroral activations and weak magnetic signatures indicate that there was a coupling between the flow burst and the ionosphere. Therefore it is unlikely that the state of the ionosphere (e.g., low value of the Pedersen conductivity) could have prohibited the growth of a full-scale substorm during the flow bursts. This leads us to suggest that the factor controlling the large-scale substorm onset was the tail configuration, not the ionospheric state.

[57] Magnetometer networks can miss or underestimate activations that are small, localized, or badly positioned far away from the observing stations, which may cause misinterpretations of the true size of the disturbance. In the event studied in this paper we assert that there were three minor auroral activations during which the magnetic disturbances were small and one substorm associated with a substorm current wedge formation. As all the events occurred over the IMAGE magnetometer network, we are quite confident that the magnitudes of the events are correctly evaluated, i.e., that the earlier auroral brightenings were not associated with large electrojet enhancement and hence substantial Joule heating.

[58] The substorm growth phase [*McPherron et al.*, 1973] was added to the original substorm definition after the realization of the importance of dayside reconnection and subsequent tail reconfiguration to the substorm process. Since then, it has been implicitely assumed that the energy consumed during the substorm comes from the energy that is stored during the growth phase. However, recent statistical studies [*Kallio et al.*, 2000; *Tanskanen et al.*, 2002] as well as this event study suggest that this is not the case. The growth phase energy is a necessary element of the substorm in that it allows reconfiguration of the magnetotail to a state where a large-scale instability can grow. However, the amount of energy that is dissipated during the expansion phase is much larger, consisting both of energy that is stored (and not previously dissipated) during the growth phase and of energy that is being transferred into the system after the substorm onset, the latter being dominant. In this scenario the expansion phase is a much more directly driven system than has been thought before: the onset requires prior energy input but the size of the substorm is determined by directly driven energy dissipation. Furthermore, if for some reason the energy input during the growth phase does not lead to reconfiguration suitable for substorm onset to occur, the magnetotail can have ways to dissipate that energy in the ionosphere (weak auroral activity, weak Joule heating) or in the magnetosphere (plasma sheet heating, kinetic Alfvén waves) [*Baumjohann et al.*, 1992; *Wygant et al.*, 2000; *Angelopoulos et al.*, 2002]. The event studied in this paper is a prime example of the fact that the energy input prior to the substorm onset is necessary only for the global configuration change (formation of a thin current sheet). If this evolution is inhibited for whatever reason, a substorm does not necessarily follow even if the energy input had been quite substantial.

[59] The substorm onset mechanism has been debated over many years. The near-Earth neutral line model proponents attribute the substorm onset to the beginning of fast reconnection in the midtail [e.g., *Baker et al.*, 1996], whereas the current disruption model advocats assume that the substorm onset occurs at the time when the near-Earth current sheet is disrupted [e.g., *Lui*, 1996]. The MHD simulation results shown in this paper tend to suggest that

Figure 10. (opposite) Time evolution of the energy content within a central part of the tail during (a) 17 December 1997 and (b) 10 December 1996. The energy contents are integrated for $Y = \pm 5\ R_E$, $Z = \pm 5\ R_E$, and $-5 > X > -15$, $-15 > X > -25$, $-25 > X > -35$, and $-35 > X > -45\ R_E$. Thermal energy (solid line), kinetic energy (dashed line), and magnetic energy (dash-dotted line) are shown separately in each panel. Average values of each curve are subtracted; the averages are for the 17 December 1997 event for $-45 < X < -35$: E(thermal) = 5.19, E(magnetic) = 4.90, and E(kinetic) = 5.10, for $-35 < X < -25$: E(thermal) = 5.93, E(magnetic) = 6.86, and E(kinetic) = 4.00, for $-25 < X < -15$: E(thermal) = 10.88, E(magnetic) = 11.62, and E(kinetic) = 4.05, for $-15 < X < -5$: E(thermal) = 31.29, E(magnetic) = 79.31, and E(kinetic) = 9.31, all in units of 10^{22} J; the averages for 10 December 1996 are for $-45 < X < -35$: E(thermal) = 5.69, E(magnetic) = 6.46, and E(kinetic) = 1.98, for $-35 < X < -25$: E(thermal) = 9.53, E(magnetic) = 8.83, and E(kinetic) = 1.61, for $-25 < X < -15$: E(thermal) = 21.29, E(magnetic) = 16.71, and E(kinetic) = 1.70, for $-15 < X < -5$: E(thermal) = 52.61, E(magnetic) = 99.10, and E(kinetic) = 5.39, all in units of 10^{22} J.

although the thin current sheet is a required component of the substorm onset, the expansion phase begins only when a large-scale flow channel forms in the middle magnetotail. However, the reason why the flows changed character from narrow, localized flows to wide, global scale neutral line is not clear from the simulation results.

[60] **Acknowledgments.** We thank N. F. Ness, C. W. Smith, and the ACE Science Center for providing the ACE magnetometer data for this study. We thank J. A. Slavin and A. Lazarus and the CDAWeb facility for the WIND magnetometer and plasma data. G. D. Reeves thanks the U. S. DOE Office of Basic Energy Science for supporting this study.

[61] Lou-Chuang Lee thanks Joel A. Fedder and another reviewer for their assistance in evaluating this paper.

References

Ahn, B.-H., S.-I. Akasofu, and Y. Kamide, The Joule heat production rate and the particle energy injection rate as a function of the geomagnetic indices AE and AL, *J. Geophys. Res.*, *88*, 6275, 1983.

Akasofu, S.-I., Energy coupling between the solar wind and the magnetosphere, *Space Sci. Rev.*, *28*, 121, 1981.

Angelopoulos, V., W. Baumjohann, C. F. Kennel, F. V. Coroniti, M. G. Kivelson, R. Pellat, R. J. Walker, H. Lühr, and G. Paschmann, Bursty bulk flows in the inner central plasma sheet, *J. Geophys. Res.*, *97*, 4027, 1992.

Angelopoulos, V., C. F. Kennel, F. V. Coroniti, R. Pellat, M. G. Kivelson, R. J. Walker, C. T. Russell, W. Baumjohann, W. C. Feldman, and J. T. Gosling, Statistical characteristics of bursty bulk flow events, *J. Geophys. Res.*, *99*, 21,257, 1994.

Angelopoulos, V., J. A. Chapman, F. S. Mozer, J. D. Scudder, C. T. Russell, K. Tsuruda, T. Mukai, T. J. Hughes, and K. Yumoto, Plasma sheet electromagnetic power generation and its dissipation along auroral field lines, *J. Geophys. Res.*, *107*(A8), 1181, doi:10.1029/2001JA900136, 2002.

Baker, D. N., S.-I. Akasofu, W. Baumjohann, J. W. Bieber, D. H. Fairfield, E. W. Hones Jr., B. Mauk, R. L. McPherron, and T. E. Moore, Substorms in the magnetosphere, in *Solar Terrestrial Physics—Present and Future*, *NASA Publ. 1120*, NASA, Washington, D.C., 1984.

Baker, D. N., T. I. Pulkkinen, V. Angelopoulos, W. Baumjohann, and R. L. McPherron, The neutral line model of substorms: Past results and present view, *J. Geophys. Res.*, *101*, 12,975, 1996.

Bargatze, L. F., D. N. Baker, R. L. McPherron, and E. W. Hoens Jr., Magnetospheric impulse response for many levels of geomagnetic activity, *J. Geophys. Res.*, *90*, 6387, 1985.

Baumjohann, W., G. Paschmann, and T. Nagai, Thinning and expansion of the substorm plasma sheet, *J. Geophys., Res.*, *97*, 17,173, 1992.

Burton, R. K., R. L. McPherron, and C. T. Russell, An empirical relationship between interplanetary conditions and Dst, *J. Geophys. Res.*, *80*, 4204, 1975.

Cowley, S. W. H., and M. Lockwood, Excitation and decay of solar wind-driven flows in the magnetosphere-ionosphere system, *Ann. Geophys.*, *10*, 110, 1992.

Crooker, N. U., G. L. Siscoe, C. T. Russell, and E. J. Smith, Factors controlling degree of correlation between ISEE 1 and ISEE 3 interplanetary magnetic field measurements, *J. Geophys. Res.*, *87*, 2224, 1982.

Dessler, A. J., and E. N. Parker, Hydromagnetic theory of geomagnetic storms, *J. Geophys. Res.*, *64*, 2239, 1959.

Dungey, J. R., Interplanetary magnetic field and the auroral zones, *Phys. Rev. Lett.*, *6*, 47, 1961.

Fairfield, D. H., and L. J. Cahill Jr., Transition region magnetic field and polar magnetic disturbances, *J. Geophys. Res.*, *71*, 155, 1966.

Fairfield, D. H., W. Baumjohann, G. Paschmann, H. Luhr, and D. G. Sibeck, Upstream pressure variations associated with the bow shock and thier effects on the magnetosphere, *J. Geophys. Res.*, *95*, 3773, 1990.

Fedder, J. A., and J. G. Lyon, The Earth's magnetosphere is 165 RE long: Or self-consistent currents, convection, magnetospheric structure and processes for northward interplanetary magnetic field, *J. Geophys. Res.*, *100*, 3623, 1995.

Fedder, J. A., J. G. Lyon, S. P. Slinker, and C. M. Mobarry, Topological structure of the magnetotail as a function of interplanetary magnetic field direction, *J. Geophys. Res.*, *100*, 3613, 1995.

Frank, L. A., J. B. Sigwarth, J. D. Craven, J. P. Cravens, J. S. Dolan, M. R. Dvorsky, P. K. Hardebeck, J. D. Harvey, and D. Muller, The Visible Imaging System (VIS) for the Polar Spacecraft, *Space Sci. Rev.*, *71*, 297–328, 1995.

Hones, E. W., Jr., T. J. Rosenberg, and H. J. Singer, Observed associations of substorm signatures at South Pole, at the auroral zone, and in the magnetotail, *J. Geophys. Res.*, *91*, 3314, 1986.

Ieda, A., S. Machida, T. Mukai, Y. Saito, T. Yamamoto, A. Nishida, T. Terasawa, and S. Kokubun, Statistical analysis of the plasmoid evolution with Geotail observations, *J. Geophys. Res.*, *103*, 4453, 1998.

Kallio, E. I. A., T. I. Pulkkinen, H. E. J. Koskinen, A. Viljanen, J. A. Slavin, and K. Ogilvie, Loading-unloading processes in the nightside ionosphere, *Geophys. Res. Lett.*, *27*, 1627, 2000.

Kauristie, K., J. Weygand, T. I. Pulkkinen, J. S. Murphree, and P. T. Newell, Size of the auroral oval: UV-ovals and precipitation boundaries compared, *J. Geophys. Res.*, *104*, 2321, 1999.

Kauristie, K., V. A. Sergeev, M. Kubyshkina, T. I. Pulkkinen, V. Angelopoulos, T. Phan, R. P. Lin, and J. A. Slavin, Ionospheric signatures of transient plasma sheet flows, *J. Geophys. Res.*, *105*, 10,677, 2000.

Klimas, A. J., D. N. Baker, D. Vassiliadis, and D. A. Roberts, Substorm recurrence during steady and variable solar wind driving: Evidence for a normal mode in the unloading dynamics of the magnetosphere, *J. Geophys. Res.*, *99*, 14,855, 1994.

Lepping, R. P., et al., The Wind magnetic field investigation, *Space Sci. Rev*, *71*, 207, 1995.

Lopez, R. E., M. Wiltberger, J. G. Lyon, C. C. Goodrich, and K. Papadopoulos, MHD simulations of the response of high-latitude potential patterns and polar cap boundaries to sudden southward turnings of the interplanetary magnetic field, *Geophys. Res. Lett.*, *26*, 967, 1999.

Lu, G., et al., Energy deposition during the January 1997 magnetic cloud event, *J. Geophys. Res.*, *103*, 11,685, 1998.

Lui, A. T. Y., Current disruption in the Earth's magnetosphere: Observations and models, *J. Geophys. Res.*, *101*, 13,067, 1996.

Lyon, J. G., R. E. Lopez, C. C. Goodrich, M. Wiltberger, and K. Papadopoulos, Simulation of the March 9, 1995 substorm: Auroral brightening and the onset of reconnection, *Geophys. Res. Lett.*, *25*, 3039, 1998.

McPherron, R. L., C. T. Russell, and M. P. Aubry, Satellite studies of magnetospheric substorms on August 15, 1968, *J. Geophys. Res.*, *78*, 3131, 1973.

Mobarry, C. M., J. A. Fedder, and J. G. Lyon, Equatorial plasma convection from global simulations of the Earth's magnetosphere, *J. Geophys. Res.*, *101*, 7859, 1996.

Nakamura, R., W. Baumjohann, V. A. Sergeev, M. Kubyshkina, M. Brittnacher, G. Parks, K. Liou, and T. Mukai, Fast flow bursts and auroral activations, in Proceedings of the Fifth International Conference on Substorms, *ESA-SP 443*, p. 319, Eur. Space Agency, Paris, July, 2000.

Ogilvie, K. W., et al., SWE, a comprehensive plasma instrument for the Wind spacecraft, *Space Sci. Rev*, *71*, 55, 1995.

Palmroth, M., T. I. Pulkkinen, and P. Janhunen, Stormtime energy transfer in global MHD simulation, *J. Geophys. Res.*, *108*(A1), 1048, doi:10.1029/2002JA009446, 2002.

Papadopoulos, K., C. Goodrich, M. WIltberger, R. Lopez, and J. G. Lyon, The physics of substorms as revealed by the ISTP, *Phys. Chem. Earth, Ser. C*, *24*, 189, 1999.

Paularena, K. I., G. N. Zastenker, A. J. Lazarus, and P. A. Dalin, Solar wind plasma correlations between IMP 8, INTERBALL-1 and WIND, *J. Geophys. Res.*, *103*, 14,601, 1998.

Perreault, P., and S.-I. Akasofu, A study of geomagnetic storms, *Geophys. J. R. Astron. Soc.*, *54*, 547, 1978.

Pulkkinen, T. I., and M. Wiltberger, Global magnetospheric response to IMF driving: ISTP observations, empirical modeling, and MHD simulations, *Phys. Chem. Earth*, *24*, 163, 1999.

Pulkkinen, T. I., and M. Wiltberger, Thin current sheet evolution as seen in observations, empirical Models and MHD simulations, *Geophys. Res. Lett.*, *27*, 1363, 2000.

Pulkkinen, T. I., D. N. Baker, R. J. Pellinen, J. Büchner, H. E. J. Koskinen, R. E. Lopez, R. L. Dyson, and L. A. Frank, Particle scattering and current sheet stability in the geomagnetic tail during the substorm growth phase, *J. Geophys. Res.*, *97*, 19,283, 1992.

Pulkkinen, T. I., D. N. Baker, L. L. Cogger, T. Mukai, and H. J. Singer, Coupling of inner tail and midtail processes, *Substorms-4*, edited by S. Kokubun and T. Kamide, p. 749, Terra Sci., Tokyo, 1998.

Raeder, J., R. L. McPherron, L. A. Frank, S. Kokubun, G. Lu, T. Mukai, W. R. Paterson, J. B. Sigwarth, H. J. Singer, and J. A. Slavin, Global simulation of the Geospace Environment Modeling substorm challenge event, *J. Geophys. Res.*, *106*, 381, 2001.

Schindler, K., and J. Birn, On the cause of thin current sheets in the near-Earth magnetotail and their possible significance for magnetospheric substorms, *J. Geophys. Res.*, *98*, 15,477, 1993.

Sckopke, N., A general relation between the energy of trapped particles and the disturbance field over the Earth, *J. Geophys. Res.*, *71*, 3125, 1966.

Sergeev, V. A., T. I. Pulkkinen, and R. J. Pellinen, Steady magnetospheric convection: A review of recent results, *Space Sci. Rev.*, *75*, 551, 1996.

Slavin, J. A., M. F. Smith, E. L. Mazur, D. N. Baker, E. W. Hones Jr., T. Iyemori, and E. W. Greenstadt, ISEE 3 observations of traveling com-

pression regions in the Earth's magnetotail, *J. Geophys. Res.*, *98*, 15,425, 1993.

Smith, C. W., J. L. Heureux, N. F. Ness, M. H. Acuna, L. F. Burlaga, and J. Scheifele, The ACE magnetic fields experiment, *Space Sci. Rev.*, *86*, 613, 1998.

Syrjäsuo, M., et al., Observations of substorm electrodynamics using the MIRACLE network, in *Substorms-4*, edited by S. Kokubun and Y. Kamide, p. 111, Terra Sci., Tokyo, 1998.

Tanskanen, E. I., T. I. Pulkkinen, H. E. J. Koskinen, and J. A. Slavin, Substorm energy budget during high and low solar activity: 1997 and 1999 compared, *J. Geophys. Res.*, *107*(A6), 1086, doi:10.1029/2001JA900153, 2002.

Troshichev, O. A., V. G. Andrezen, S. Vennerstroem, and E. Friis-Christensen, Magnetic activity in the polar cap: A new index, *Planet. Space Sci*, *36*, 1095, 1988.

Tsyganenko, N. A., Magnetospheric magnetic field model with a warped tail current sheet, *Planet. Space Sci.*, *37*, 5, 1989.

Turner, N. E., D. N. Baker, T. I. Pulkkinen, J. L. Roeder, J. F. Fennell, and V. K. Jordanova, Energy content in the stormtime ring current, *J. Geophys. Res.*, *106*, 19,149, 2001.

Vassiliadis, D. V., A. J. Klimas, D. N. Baker, and D. A. Roberts, A description of solar wind-magnetosphere coupling based on nonlinear filters, *J. Geophys. Res.*, *100*, 3495, 1995.

Vennerstroem, S., E. Friis-Christensen, O. A. Troshichev, and V. G. Andrezen, Comparison between the polar cap index PC and the auroral electrojet indices AE, AL, adn AU, *J. Geophys. Res.*, *96*, 101, 1991.

Wiltberger, M., T. I. Pulkkinen, J. G. Lyon, and C. C. Goodrich, MHD simulation of the magnetotail during the December 10, 1996 substorm, *J. Geophys. Res*, *105*, 27,649, 2000.

Wygant, J. R., et al., Polar spacecraft based comparisons of intense electric fields and Poynting flux near adn within the plasma sheet-tail lobe boundary to UVI images: An energy source for the aurora, *J. Geophys. Res.*, *105*, 18,675, 2000.

T. I. Pulkkinen and E. I. Tanskanen, Finnish Meteorological Institute, P.O. Box 503, FIN-00101 Helsinki, Finland. (tuija.pulkkinen@fmi.fi; etanskanen@lepvax.gsfc.nasa.gov)

L. A. Frank and J. B. Sigwarth, Department of Physics and Astronomy, The University of Iowa, Iowa City, IA 52242-1479, USA. (frank@iowasp.physics.uiowa.edu; sigwarth@iowasp.physics.uiowa.edu)

T. Nagai, Department of Earth and Planetary Sciences, Tokyo Institute of Technology, Tokyo 152, Japan. (nagai@geo.titech.ac.jp)

G. D. Reeves, Mail Stop D-436, Los Alamos National Laboratory, Los Alamos, NM 87545, USA. (reeves@lanl.gov)

J. A. Slavin, NASA Goddard Space Flight Center, Code 696, Greenbelt, MD 20771, USA. (slavin@lepjas.gsfc.nasa.gov)

M. Wiltberger, Department of Physics and Astronomy, Dartmouth College, 6127 Wilder Laboratory, Hanover, NH 03755, USA. (wiltbemj@tinman.dartmouth.edu)

Figure 5. Polar/VIS images of the auroral oval during 17 December 1997.

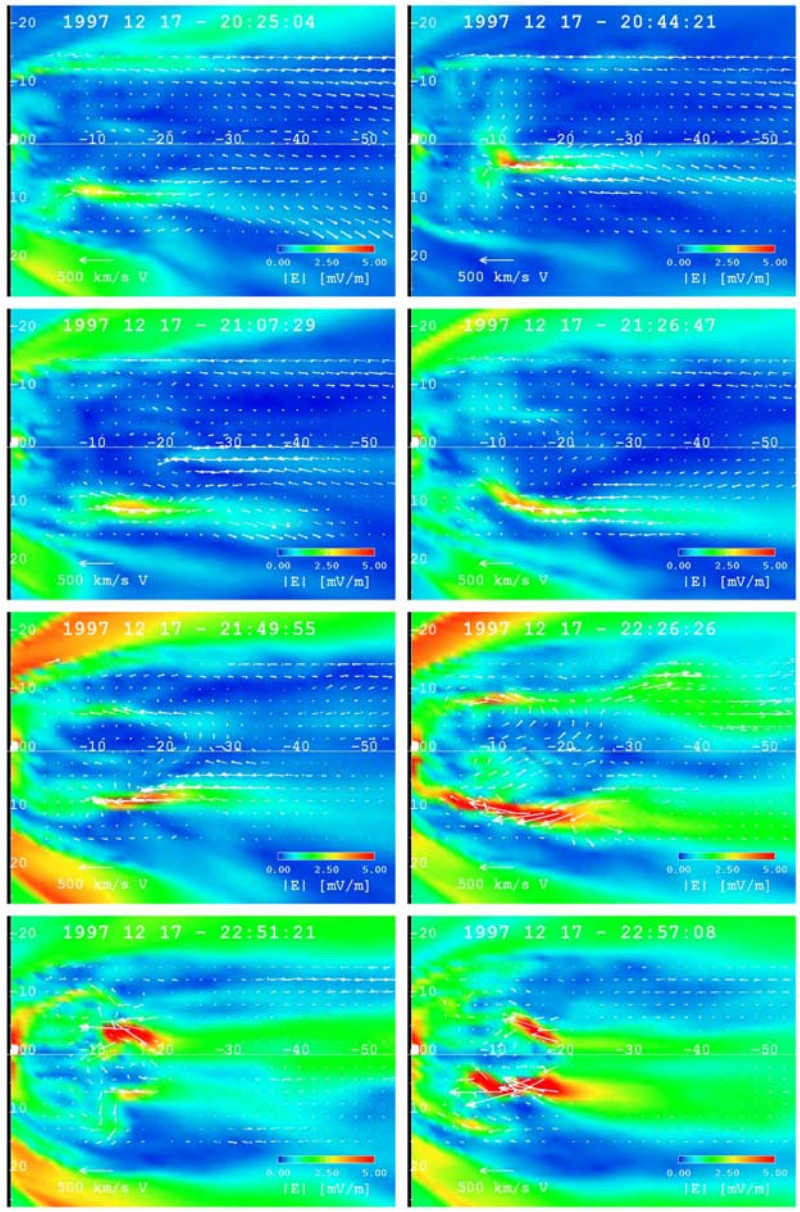

Figure 7. Electric field in the plane $Z = -3.5\ R_E$ from the MHD simulation. The white arrows show the flow velocity projected to the equatorial plane. Time runs from left to right and from top to bottom, the frames are taken at 2025, 2044, 2107, 2126, 2149, 2226, 2251, and 2257 UT.

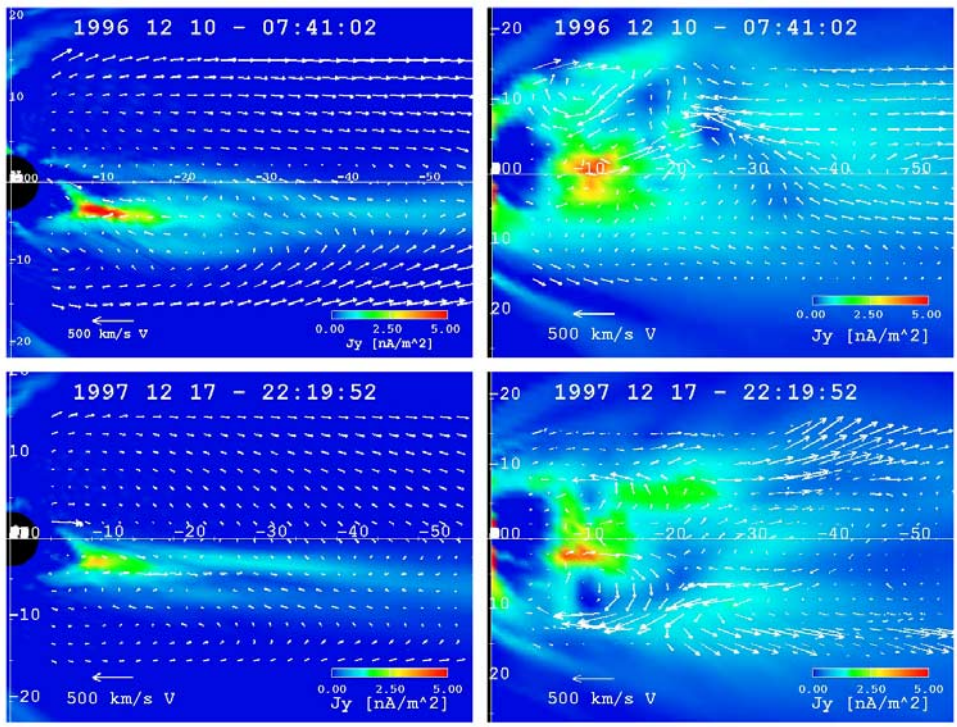

Figure 9. Electric current density in the (left) noon-midnight plane and in the (right) $Z = const$ plane near the plasma sheet center for (top) 10 December 1996 substorm event and (bottom) 17 December 1997 event.